Title

TRIANGULAR CURRENT-SWEEP CHRONOPOTENTIOMETRY AT ROTATING DISK AND STATIONARY, PLANAR ELECTRODES

Authors

Verbrugge, M.W.
Tobias, C.W.

Publication Date

1985

Lawrence Berkeley Laboratory
UNIVERSITY OF CALIFORNIA

Materials & Molecular Research Division

Submitted to Journal of Electroanalytical Chemistry and Interfacial Electrochemistry

TRIANGULAR CURRENT-SWEEP CHRONOPOTENTIOMETRY AT ROTATING DISK AND STATIONARY, PLANAR ELECTRODES

M.W. Verbrugge and C.W. Tobias

January 1985

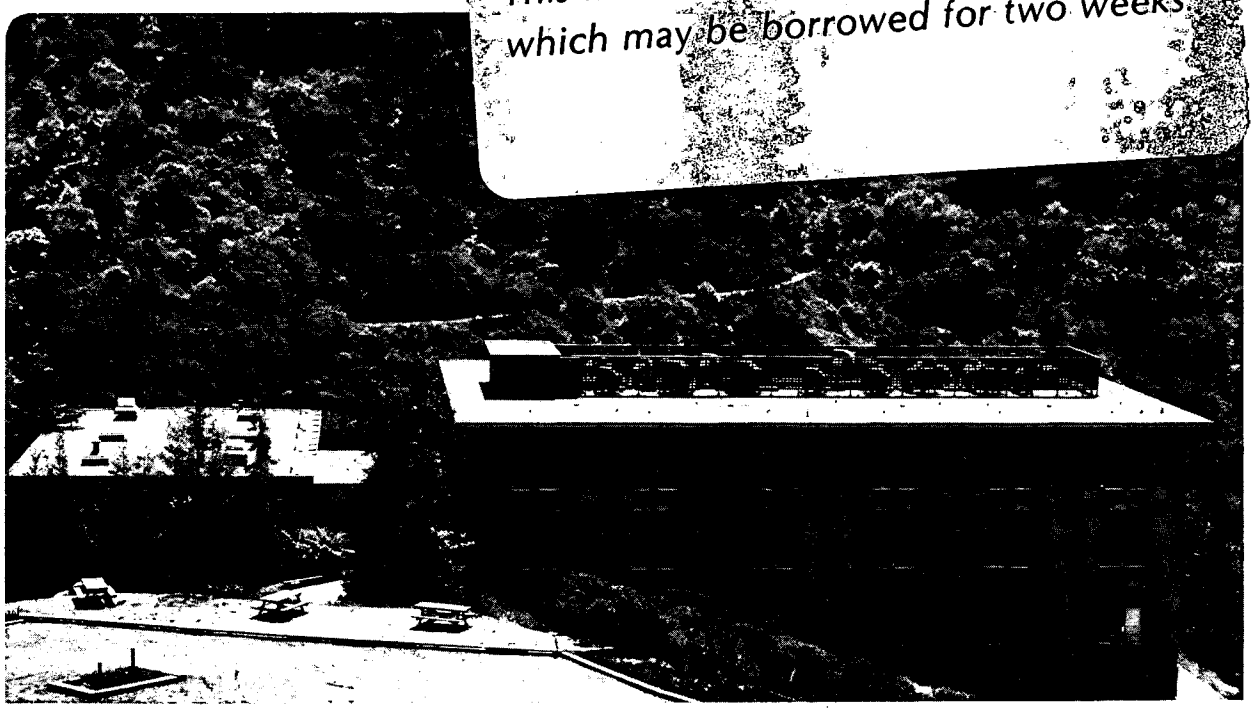

Prepared for the U.S. Department of Energy under Contract DE-AC03-76SF00098

DISCLAIMER

LBL-19029

TRIANGULAR CURRENT-SWEEP CHRONOPOTENTIOMETRY AT ROTATING DISK AND STATIONARY, PLANAR ELECTRODES

by

Mark W. Verbrugge and Charles W. Tobias

Lawrence Berkeley Laboratory
University of California
Berkeley, California 94720

This work was supported by the Director,
Office of Energy Research, Office of Basic Energy Sciences,
Materials Sciences Division of the Office of the
U.S. Department of Energy, under Contract No. DE-AC03-76SF00098

TRIANGULAR CURRENT-SWEEP CHRONOPOTENTIOMETRY AT ROTATING DISK AND STATIONARY, PLANAR ELECTRODES

Mark W. Verbrugge and Charles W. Tobias

Lawrence Berkeley Laboratory
University of California
Berkeley, California 94720

Abstract

A convenient series solution is presented for the evaluation of reactant and product concentrations during triangular current-sweep chronopotentiometry at a rotating disk electrode, and at a stationary, planar electrode in the absence of free convection. The advantages of controlled-current processes, relative to controlled-potential processes, for obtaining kinetic, thermodynamic, and transport information are elucidated. Theoretical predictions are compared with results obtained for the deposition of cadmium from a dilute, aqueous, cadmium-sulfate/potassium-sulfate electrolyte. A multidimensional optimization routine, the Levenberg-Marquardt algorithm, is used to evaluate parameters.

Introduction

In the study of pulsed-electrolysis processes, the question arises: Can one more conveniently obtain kinetic, thermodynamic, and transport information by controlling the potential or the current? In chronoamperometric experiments, the potential is a programmed function and the current is a dependent variable. This method has the advantage of using the reversible cell potential, an easily calculated value, as a reference point. In chronopotentiometric experiments, the current is a programmed function and the potential is a dependent variable. The relevant diffusion-limited current and zero current represent two references.

If mathematical difficulties are not considered, exactly the same amount of information can be gained from either chronopotentiometric or chronoamperometric experiments. The same number of system parameters and variables exist and the same equations describe the processes. Because of the availability of high-speed computers, the argument concerning which is the better of the methods is somewhat dated. If, however, a multidimensional optimization routine is to be used to obtain a best fit of experimental data, it is necessary that an efficient solution be available for the mass-transfer problem.

Potential-controlled processes are usually more difficult to describe mathematically. In this case, a complicated boundary condition relating the cell current, electrode potential, and ionic surface concentrations of the reactant and product species must be introduced to link the controlled potential to the mass-transport problem. For current-controlled processes, on the other hand, the mass-transport problem avoids kinetic considerations, provided only one electrochemical reaction takes place.

For the mass-transfer problems we solve in this work, the partial differential equations are linear; hence, we are able to express the differential

equations and the boundary conditions as an integral by making use of Laplace transforms, or, as is done in this work, by Duhamel's theorem. In the analysis of the linear systems used to describe the chronoamperometric or chronopotentiometric processes, either the cell current or the surface concentrations are included in the resulting integral. For controlled-current processes, the cell current is specified. For controlled-potential processes, however, the kinetic equation does not generally yield an explicit expression for the surface concentration or the cell current. The following mathematical analysis will make this point more clear.

The effects of double-layer charging, migration, and a non-uniform potential field are neglected in this treatment. The experiments reported on in this work were designed to minimize these effects, to demonstrate the applicability of the theoretical results, and to study the technologically important cadmium deposition process.

Triangular Current-Sweep Chronopotentiometry at an SPE

Fick's second law, the diffusion equation, is used to describe the transport of reactants and products:

$$\frac{\partial c_i}{\partial t} = D_i \frac{\partial^2 c_i}{\partial y^2} \qquad [1]$$

The initial condition is uniform concentration,

$$c_i(0,y) = c_i^{\infty} \ , \qquad [2]$$

and the two boundary conditions are bulk concentration of species far from the electrode,

$$c_i(t,\infty) = c_i^{\infty} \ , \qquad [3]$$

and Faraday's law relating the concentration gradient at the electrode surface to the programmed current function

$$\frac{\partial c_i(t,0)}{\partial y} = \frac{s_i i(t)}{nFD_i} \quad . \qquad [4]$$

The electrode reaction is written as

$$ne^- \underset{k_a}{\overset{k_c}{\rightleftharpoons}} \sum_i s_i M_i^{z_i} \qquad [5]$$

For $s_i > 0$, the species is an anodic reactant. For $s_i < 0$, the species is a cathodic reactant.

The triangular-sweep function $i(t)$ can be expressed by a Fourier series (1)

$$i(t) = i_I + (i_{II} - i_I)\left(\frac{1}{2} - \frac{4}{\pi^2}\sum_{j=1,3,\ldots}^{j=\infty}\frac{1}{j^2}\cos\frac{j\pi t}{L}\right). \qquad [6]$$

This programmed current density is depicted in Fig. 1.

Using Duhamel's theorem, Eqs. [1] - [4] can be replaced by

$$c_i^{surf} - c_i^{\infty} = -\frac{s_i}{nF\sqrt{\pi D_i}}\int_0^t i(\lambda)(t-\lambda)^{-\frac{1}{2}}d\lambda \quad . \qquad [7]$$

This equation, derived in the Appendix, has appeared numerous times in the SPE chronopotentiometry literature. (2-7) Two reviews (8,9) also cover the SPE literature.

Substituting Eq. [6] into Eq. [7] and performing the integration, the following solution can be obtained:

$$\frac{c_i^{surf}}{c_i^{\infty}} = 1 - \frac{s_i(i_{II} - i_I)}{nFc_i^{\infty}}\left(\frac{L}{\pi D_i}\right)^{\frac{1}{2}}\left\{\left[1 + \frac{i_I}{2(i_{II} - i_I)}\right]\left(\frac{t}{L}\right)^{\frac{1}{2}} - \frac{8}{\pi^2}\sum_{j=1,3,\ldots}^{j=\infty}\frac{1}{\sqrt{2j^5}} \times \right. \quad [8]$$

$$\left.\left[\cos\left(\frac{j\pi t}{L}\right)C_F\left(\sqrt{2jt/L}\right) + \sin\left(\frac{j\pi t}{L}\right)S_F\left(\sqrt{2jt/L}\right)\right]\right\}$$

The functions C_F and S_F are Fresnel integrals. They are tabulated, and the following expressions can be used to evaluate them: (10)

$$C_F(x) = \frac{1}{2} + f(x)\sin\left(\frac{\pi}{2}x^2\right) - g(x)\cos\left(\frac{\pi}{2}x^2\right) \quad [9]$$

$$S_F(x) = \frac{1}{2} - f(x)\cos\left(\frac{\pi}{2}x^2\right) - g(x)\sin\left(\frac{\pi}{2}x^2\right) \quad [10]$$

$$f(x) = \frac{1 + 0.926x}{2 + 1.792x + 3.104x^2} + \epsilon(x) \quad [11]$$

$$g(x) = \frac{1}{2 + 4.142x + 3.492x^2 + 6.670x^3} + \epsilon(x) \quad [12]$$

$$|\epsilon(x)| \leq 0.002$$

For values of t greater than L, C_F and S_F rapidly approach $\frac{1}{2}$. The concentration expression can be further simplified since a relatively accurate answer is obtained if only the $j = 1$ term is kept in the series. This is shown in Fig. 2, where a plot of the surface concentration is given. With these approximations, and for $i_I = 0$, the concentration expression simplifies to

$$\frac{(c_i^{\infty} - c_i^{surf})nF'}{s_i i_{II}}\left(\frac{\pi D_i}{L}\right)^{\frac{1}{2}} = \left(\frac{t}{L}\right)^{\frac{1}{2}} - \frac{2\sqrt{2}}{\pi^2}\left[\cos\left(\frac{\pi t}{L}\right) + \sin\left(\frac{\pi t}{L}\right)\right]. \quad [14]$$

Equation [14] represents a satisfying result of this work. The relatively cumber-

some mathematical description of the SPE system has been simplified to yield a compact and accurate solution for the surface concentrations. It is evident that the concentration oscillates about the value corresponding to a current step to $\frac{i_{II}}{2}$, the average current density for the process.

Triangular Current-Sweep Chronopotentiometry at an RDE

Current-controlled electrolysis at an RDE has received a great deal of attention. (11-20) In a general treatment for the RDE system incorporating both radial and axial variations in concentration and potential, dimensionless groups arise which contain the disk radius, rotation rate, current density, and other transport and kinetic parameters. (13) Experiments can be easily constructed to remove radial effects (14), as can be seen by an analysis of the appropriate dimensionless groups. For experimental conditions consisting of a small disk, low reactant and product concentrations, and a well supported electrolyte, a one-dimensional treatment (excluding radial variations) can be used to rigorously and fundamentally analyze the RDE system. In the present work, a one-dimensional convective-diffusion equation is used to model the transport of the reactants and products:

$$\frac{\partial c_i}{\partial t} + v_y \frac{\partial c_i}{\partial y} = D_i \frac{\partial^2 c_i}{\partial y^2} \qquad [15]$$

The velocity normal to the disk surface is given by (21,22)

$$v_y = -0.51023\,\omega^{\frac{3}{2}} \nu^{-\frac{1}{2}} y^2 \,. \qquad [16]$$

The initial and boundary conditions are given by Eqs. [2], [3], and [4]. The electrode reaction is given by Eq. [5] and the current density is expressed in Eq. [6].

To obtain a solution, an integral analogous to Eq. [7] is required. In their

classic treatment, Rosebrugh and Lash Miller (11) obtained such an integral for the case of pure diffusion, which can be modeled by Eqs. [1] (the diffusion equation), [2], [4], and the boundary condition

$$c_i(y,\delta_i) = c_i^{\infty} \quad . \qquad [17]$$

where δ_i represents the thickness of a stagnant diffusion layer. Pesco and Cheh have made use of this approach to model periodic-current chronopotentiometry at an RDE. (20)

The convective-diffusion equation, Eq. [15], subject to the conditions given by Eqs. [2], [3], and [4] can be replaced by the following superposition integral. (15,23)

$$c_i(\theta_i,\zeta_i) - c_i^{\infty} = \int_0^{\theta_i} \frac{\partial c_i(\lambda,0)}{\partial \zeta_i} \frac{\partial}{\partial \lambda} \Theta_{F,i}(\theta_i - \lambda,\zeta_i) d\lambda \quad . \qquad [18]$$

The new variables are

$$\theta_i = \frac{D_i t}{\delta_i^2} \quad , \qquad [19]$$

$$\delta_i = \left(\frac{3D_i}{0.51023\nu}\right)^{\frac{1}{3}} \left(\frac{\nu}{\omega}\right)^{\frac{1}{2}} \quad , \qquad [20]$$

$$\zeta_i = \frac{y}{\delta_i} \quad , \text{ and} \qquad [21]$$

$$\Theta_{F,i} = \frac{c_i}{\left[\frac{\partial c_i(\theta,0)}{\partial \zeta_i}\right]} \quad . \qquad [22]$$

In contrast to the SPE system, the RDE system has a characteristic length δ_i, which is representative of the the region where the concentration differs from c_i^{∞}; however, the convective-diffusion equation is used to model the transport,

and δ_i is used only to nondimensionalize the problem. Since the SPE system has no characteristic length, the complete mass-transfer solution can be displayed in Fig. 2 by a single curve. Such a convenient plot for the RDE system cannot be constructed.

The dimensionless concentration function $\Theta_{F,i}$ results from the flux-step problem, described by the convective-diffusion equation, along with conditions [2], [3], and a flux-step for the last boundary condition. The solution for the flux-step problem is

$$\Theta_{F,i} = \int_{\zeta_i}^{\infty} e^{-x^3}\,dx - \sum_{k=0}^{k=\infty} B_k Z_k(\zeta_i) e^{-b_k \theta_i} \quad . \qquad [23]$$

Equations [18] and [23] result from the work of Nisancioglu and Newman. The values of B_k and b_k are given in the Appendix. At the electrode surface, the eigenfunction Z_k is equal to unity. Using Fick's law, the normal gradient $\frac{\partial c_i}{\partial \zeta_i}$ in Eq. [18] can be related to the current density $i(t)$. After combining Eqs. [6], [18], and [23] and integrating, the following expression can be obtained for the concentrations

$$\frac{(c_i^{\infty} - c_i) n F D_i}{s_i (i_{II} - i_I)} = \left(\frac{1}{2} + \frac{i_I}{i_{II} - i_I}\right) \sum_{k=0}^{k=\infty} B_k Z_k (1 - e^{-b_k \theta_i}) - \frac{4}{\pi^2} \sum_{k=0}^{k=\infty} b_k B_k Z_k \sum_{j=1,3,\ldots}^{j=\infty} \qquad [24]$$

$$\frac{1}{j^2 \left[b_k^2 + \left(\frac{j\pi}{\theta_{L,i}} \right)^2 \right]} \left\{ b_k \cos\left(\frac{j\pi\theta_i}{\theta_{L,i}} \right) \left[1 + e^{-b_k \theta_i} \left\{ \left(\frac{j\pi}{b_k \theta_{L,i}} \right) \sin\left(\frac{j\pi\theta_i}{\theta_{L,i}} \right) - \cos\left(\frac{j\pi\theta_i}{\theta_{L,i}} \right) \right\} \right] \right.$$

$$+\left(\frac{j\pi}{\theta_{L,i}}\right)\sin\left(\frac{j\pi\theta_i}{\theta_{L,i}}\right)\left[1-e^{-b_k\theta_i}\left\{\left(\frac{b_k\theta_{L,i}}{j\pi}\right)\sin\left(\frac{j\pi\theta_i}{\theta_{L,i}}\right)+\cos\left(\frac{j\pi\theta_i}{\theta_{L,i}}\right)\right\}\right]\Bigg)$$

where $\theta_{L,i}=\dfrac{D_i L}{\delta_i^2}$.

This solution can be considerably simplified. At the electrode surface, $Z_k = 1$. For $i_I = 0$ and long times, the solution can be further reduced to

$$\frac{(c_i^{\infty}-c_i^{surf})nFD_i}{s_i i_{II}}=\frac{1}{2}\Gamma\left(\frac{4}{3}\right)-\frac{4}{\pi^2}\sum_{k=0}^{k=\infty}b_k B_k\sum_{j=1,3,\ldots}^{j=\infty}\frac{1}{j^2\left[b_k^2+\left(\frac{j\pi}{\theta_{L,i}}\right)^2\right]}\times \qquad [25]$$

$$\left[b_k\cos\left(\frac{j\pi\theta_i}{\theta_{L,i}}\right)+\left(\frac{j\pi}{\theta_{L,i}}\right)\sin\left(\frac{j\pi\theta_i}{\theta_{L,i}}\right)\right].$$

As was observed for the SPE system, this solution oscillates about the solution for a current step to $\dfrac{i_{II}}{2}$, the average current density during the process.

The Current-Potential Expression

The most accessible experimental variables are the total cell current and the potential of the working electrode with respect to a suitable reference. We shall therefore relate the predicted concentrations to the programmed current density and the measured potential by a Butler-Volmer kinetic expression

$$\frac{i}{nF}=k_a e^{(1-\beta)nfV}\prod_i a_i^{s_i}-k_c e^{-\beta nfV}\prod_i a_i^{-s_i}\ , \qquad [26]$$

where $f=\dfrac{F}{RT}$, a_i represents the activity of species i, and

$$V = E + \left[U^{\theta}_{ref} - \frac{1}{n_{ref} f} \sum_i s_{i,ref} \ln a_{i,ref} \right] - ir \quad . \qquad [27]$$

The bracketed term in Eq. [27] represents the open-circuit potential difference between the reference electrode and a standard hydrogen electrode (SHE). E is the measured potential between the working electrode and the reference electrode. The last term in Eq. [27] accounts for the ohmic drop between the working electrode and the reference electrode. Therefore, the potential difference between the working electrode and a SHE, corrected for ohmic drop, is represented by V.

For dilute solutions, the activities in Eq. [26] can be replaced by concentrations. For the discharge of a metal ion ($a_{solid} = 1$) in a dilute system with negligible ohmic drop, Eqs. [26] and [27] can be combined to yield

$$\frac{i}{nF} = k_a e^{(1-\beta)nfE} - k_c e^{-\beta nfE} \left(\frac{c_i^{surf}}{\rho_o} \right) . \qquad [28]$$

The SHE has been taken as a reference, and a first-order reaction has been assumed. Since a SHE has been assumed, the bracketed term in Eq. [27] is zero. It should be noted that the concentration overpotential is included in this treatment since the surface concentration of the discharging metal ion is used. Equation [28] contains two independent kinetic parameters, β and the magnitude of either k_c or k_a . The Gibbs free energy of reaction fixes the ratio $\frac{k_c}{k_a}$.

In this work, the electrodeposition of cadmium from dilute, aqueous, $CdSO_4 - K_2SO_4$ solutions has been chosen to test the viability of the theoretical model. The deposition of cadmium from a well supported, aqueous electrolyte, a technologically important process, has been studied by a number of authors. (24-31) It is not clear whether a one-step mechanism,

$$Cd^{2+} + 2e^- \underset{k_a}{\overset{k_c}{\rightleftharpoons}} Cd \qquad [29]$$

described by Eq. [28], or a two-step mechanism, involving a Cd^+ species, should be used to capture the salient features of the kinetic behavior. (25,26,29,30,31)

Since the Cd^+ species has never been shown to exist as a stable ion in solution, let us postulate that Cd^+ is adsorbed at the electrode surface. The proposed mechanism is:

$$Cd^{2+} + e^- \underset{k_{a,1}}{\overset{k_{c,1}}{\rightleftharpoons}} Cd^+_{ads} \qquad [30]$$

$$Cd^+_{ads} + e^- \underset{k_{a,2}}{\overset{k_{c,2}}{\rightleftharpoons}} Cd \qquad [31]$$

This mechanism appears in the metal-deposition literature for other metal/metal-ion systems. (22,26) Using our nomenclature, the current-potential expression for the two-step process, given by Eqs. [30] and [31], (referred to with subscripts 1 and 2, respectively) is

$$\frac{i}{2F} = \frac{k_{a1}k_{a2}e^{(2-\beta_1-\beta_2)fE} - k_{c1}k_{c2}e^{-(\beta_1+\beta_2)fE}\left(\frac{c^{surf}_{Cd^{2+}}}{\rho_o}\right)}{k_{c2}e^{-\beta_2 fE} + k_{a1}e^{(1-\beta_1)fE}} \qquad [32]$$

In writing Eq. [32], it is assumed that the time rate of change of the current is slow enough to allow reactions 1 and 2 to occur at the same rate ($i_1 = i_2 = \frac{i}{2}$), since the Cd^+_{ads} ions do not diffuse away from the electrode surface. For this reason, our experiments were conducted at relatively low frequencies. It should be

noted that for $k_{c2} \gg k_{a1}$ or $k_{c2} \ll k_{a1}$, an apparent one-step current-potential expression results. We also have

$$\Delta G_1^\theta = FU_1^\theta = RT \ln \frac{k_{c1}}{k_{a1}} \text{ , and} \qquad [33]$$

$$\Delta G_2^\theta = FU_2^\theta = RT \ln \frac{k_{c2}}{k_{a2}} \text{ ;} \qquad [34]$$

and hence

$$U_1^\theta + U_2^\theta = -0.403 \; volts, \qquad [35]$$

the standard electrode potential for the reduction of Cd^{2+} to Cd. In Eqs. [33] and [34], the rate constants need not have the same units since the standard state activities of the products and reactants are also included in these expressions. The standard state activities, however, are unity for the solid state (a mole fraction of unity) and the electrolyte species (1 molal).

Equation [32] has five independent parameters: β_1, β_2, k_{c1}, k_{c2}, and U_1^θ. The ratios of the rate constants are fixed by Eqs. [33] and [34]. The sum $U_1^\theta + U_2^\theta$ is fixed by Eq. [35].

Neither Eq. [28] nor Eq. [32] can be solved explicitly for E. A Newton-Raphson routine which converges rapidly for each equation is outlined in the Appendix.

Experimental

The experiments described below were designed to illustrate the utility of triangular current-sweep chronopotentiometry. We have chosen the deposition of cadmium because of its technological importance and because it offered two key advantages: the hydrogen overvoltage is very high on this metal, and cadmium ions are not complexed in the aqueous, potassium-sulfate electrolyte

employed in this study.

A 5-mm-diameter, glassy-carbon disk electrode was employed in our experiments. Standard metallographic polishing techniques were used to remove all projections greater than one micron in height. The potential of the working electrode was measured against a mercury-mercurous sulfate reference electrode. For the RDE experiments, a Pine Instruments ASRP2 rotator was used. The Princeton Applied Research model 173 potentiostat/galvanostat controlled the operation of the cell. An Interstate F77 function generator was used with the potentiostat/galvanostat. The data were stored on a Nicolet 1090A digital oscilloscope and later transferred to an HP9825 computer.

The electrolyte, a $0.0058-M-CdSO_4$ / $0.25-M-K_2SO_4$ solution, was prepared from analytical reagent grade chemicals and distilled water which was passed through a Culligan water purification unit consisting of an organic trap, a deionizer, and a microfilter. The specific conductance of the treated water was 15 Mohm-cm. Nitrogen, first equilibrated with a similar electrolyte, was bubbled through the cell solution for 1 hour prior to experiments. A nitrogen atmosphere was maintained above the electrolyte during the experiment. The temperature was maintained at 25 $^{\circ}C$. Handbook values were used for the solvent density ρ_o ($0.001 \frac{kg}{cm^3}$) and the kinematic viscosity ν ($0.01 \frac{cm^2}{sec}$).

The diffusion coefficient of Cd^{2+}, $3.6 \times 10^{-6} \frac{cm^2}{sec}$, was calculated from the limiting current curves depicted in Fig. 3. The resulting Levich plot is shown in Fig. 4. The line drawn through the points in Fig. 4 was obtained by the method of least squares; the origin was not included in the linear regression.

Discussion

We have chosen a Levenberg-Marquardt algorithm to compare and contrast the theoretically predicted electrode potentials with the experimentally

measured results. One basic algorithm for finding a minimum is the method of steepest descent, which goes back to Cauchy and his attempts to solve the problem of finding a minimum of a real-valued, multivariable function by repeatedly finding minima of a function of one variable. Alternatively, the Newton-Raphson algorithm can be used to vary the parameters until the partial derivatives of the objective function $\sum_k (E_{k,theory} - E_{k,experiment})^2$ with respect to the parameters to be optimized are sufficiently close to zero. The Newton-Raphson method is often seen to diverge from the solution, while the method of steepest descent converges in an agonizingly slow and computationally expensive fashion. Levenberg (32) proposed a method to intelligently estimate a damping factor for the Newton-Raphson routine, while preserving the symmetry of the problem in order that simplified methods for the solution of linear, simultaneous equations could still be employed. Marquardt (33) proposed another modification which allowed a proper scaling of the problem by making use of the standard deviations of the partial derivatives in the Jacobian. Marquardt used a *maximum neighborhood* method which performs an optimum interpolation between the Newton-Raphson method and the method of steepest descent. The Levenberg-Marquardt routine we used was written by Garbow, Hillstrom, and More. (34) Another more recent method, the Simplex algorithm (35,36) is appealing; however, it does not converge as quickly as a Levenberg-Marquardt algorithm, which avoids the divergence problems of the Newton-Raphson without incurring unacceptable losses in speed. Three experiments, each with fifty data points, were used as data bases in the optimization program. Typically, the program used less than 500 CP seconds on a CDC 7600 computer.

Results obtained from the RDE system were used to compare experiment and theory. With this system, natural convection, spherical diffusion, and one-micron surface roughness will not be important considerations. This is less

often the case for the SPE system.

After optimizing the two parameters for Eq. [28] and the five parameters for Eq. [32], we obtained an unexpected result. The best fit obtained with the five-parameter model was exactly identical to the best fit obtained with the two-parameter model. A number of initial guesses were attempted to ensure that the fit solution was indeed a global minimum. In addition, the logarithms of the rate constants were used in the optimization routine to speed convergence.

We originally introduced the two-step mechanism to ascertain whether it could better represent the cusp in the potential-time data shown at $\frac{t}{2L} = 0.25$ in Fig. 7. Since the data could not be better represented by the two-step mechanism, and since there is no physical evidence for the presence of Cd^+, we prefer the use of Eq. [28], representing the single-step charge transfer, for the current-potential relation. The optimized results, however, cannot be used to refute the two-step mechanism because it is possible that the kinetic constants for the one-step process represent lumped parameters. The optimized parameters are:

$$\beta = 0.5707$$

$$k_c = 6.991 \times 10^{-17}$$

These parameters can be used to calculate an exchange-current density:

$$i_o = nF k_a^{\beta} k_c^{1-\beta} a_{Cd}^{\beta} (c_{Cd^{2+}}^{\infty})^{1-\beta}$$

For the pure cadmium electrode, $a_{Cd} = 1$. The above equation can be used to calculate $i_o = 0.0897 \frac{mA}{cm^2}$. Vetter has cited (37) values of $\beta = 0.55$ and $i_o = 1.5 \frac{mA}{cm^2}$ for a similar $0.005 - M - CdSO_4 / 0.8 - M - K_2SO_4$ electrolyte, cadmium-electrode system at $20\,^{\circ}C$. The exchange-current densities differ by

an order of magnitude, although the symmetry factors show close agreement.

The kinetic parameters can be used to calculate the appropriate dimensionless groups to verify the one-dimensional nature of the mass transport in the experiments. These calculations were made, and we conclude that the one-dimensional analysis, stated explicitly by Eq. [15], is a correct representation for this experimental system.

Calculated potential-time curves for the single-step, two-parameter mechanism are compared with experiment in Figs. 5, 6 and 7. Figure 8 displays the surface concentration during the higher frequency experiment. The results for the five-parameter model could not be distinguished from the results for the two-parameter model. The uppermost curve in each figure represents the potential response which would result in the absence of kinetic resistance. These results represent the uniform and sustained periodic state; hence, Eq. [25] can be used to obtain the surface concentrations. When $\frac{t}{2L} = 0$, the current density is i_I. For $\frac{t}{2L} = 0.5$, the current density is i_{II}. In these experiments, $i_I = 0$ and $i_{II} = -1.53\ \frac{mA}{cm^2}$. The low-frequency results are shown in Figs. 5 and 6. Both the model and experimental results display a pseudosteady state. For the low frequency cases, the concentration $c_{Ox,i}^{surf}$ is lowest halfway through the cycle, when $i = i_{II}$. Correspondingly, the concentration overpotential has its largest magnitude at midcycle. This is particularly apparent in Fig. 5.

The slightly higher frequency results are shown in Figs. 7 and 8. Fig. 7 has a an asymmetric nature relative to Figs. 5 and 6, because the characteristic time L for the current sweep is of the same order of magnitude as the characteristic time $\frac{\delta_i^2}{D_i}$ for the mass transport. The corresponding concentration profile shown in Fig. 8 is asymmetric as well.

Conclusions

Convenient mass-transfer solutions have been obtained for triangular current-sweep chronopotentiometry at rotating disk and stationary, planar electrodes in the absence of free convection. Because the solutions can be evaluated efficiently, a numerical multidimensional-optimization routine, which requires a large number of functional evaluations, was used to compare and contrast the ability of various discharge mechanisms to match experimental data. Using the rotating disk system, we have examined the cadmium electrodeposition process. For a single-step, two-electron transfer mechanism, the optimized exchange-current density (based on the bulk concentration of Cd^{2+}) and the symmetry factor are 0.0897 $\frac{mA}{cm^2}$ and 0.571, respectively.

Acknowledgement

This work was supported by the Director, Office of Energy Research, Office of Basic Energy Sciences Division of the Office of the U.S. Department of Energy, under Contract No. DE-AC03-76SF00098.

Nomenclature

a	activity
c	concentration, $\frac{moles}{cm^3}$
E	measured electrode potential, *volts*
D	diffusion coefficient, $\frac{cm^2}{sec}$
e^-	symbol for the electron
i	current density, $\frac{A}{cm^2}$
i_o	exchange-current density, $\frac{A}{cm^2}$
i_I, i_{II}	current densities defined in Fig. 1, $\frac{A}{cm^2}$
F	Farraday's constant, $\frac{C}{equivalent}$
G^θ	standard free energy of reaction, $\frac{J}{mole}$
k_a, k_c	anodic and cathodic rate constants
L	one-half the cycle period, *sec*
M_i	symbol for the chemical formula of species i
n	number of electrons in a reaction
r	cell resistance multiplied by the disk area, $\Omega-cm^2$
R	universal gas constant, 8.314 $\frac{J}{mole-K}$
s	stoichiometric coefficient
T	absolute temperature, K
t	time, *sec*
V	electrode potential defined by Eq. 27, *volts*

v_y velocity normal to the electrode surface, $\frac{cm}{sec}$

U^0 standard electrode potential, *volts*

y distance normal to the electrode surface, *cm*

z charge number

Greek letters

β symmetry factor

δ characteristic length, *cm*

ζ dimensionless distance

Θ_F dimensionless concentration

θ dimensionless time

θ_L dimensionless half-cycle time

$\Gamma(4/3)$ the gamma function of 4/3

λ dummy variable of integration, *sec*

ν kinematic viscosity, $\frac{cm^2}{sec}$

π 3.1415...

ρ_o solvent density, $\frac{kg}{cm^3}$

Subscripts

i species i

ref reference electrode compartment

1,2 reactions 1 and 2

Superscripts

surf electrode surface

∞ far away from the electrode surface

Appendix

Duhamel's Integral for the SPE

The flux-step (or current-step) problem is given by the diffusion equation,

$$\frac{\partial c_i}{\partial t} = D_i \frac{\partial^2 c_i}{\partial y^2} \ , \qquad \text{[A-1]}$$

subject to an initial condition representing initially uniform concentration,

$$c_i(0,y) = c_i^{\infty} \ , \qquad \text{[A-2]}$$

a boundary condition for bulk concentration of species far from the electrode,

$$c_i(t,\infty) = c_i^{\infty} \ , \qquad \text{[A-3]}$$

and a second boundary condition relating the current density to the concentration gradient at the electrode surface by Farraday's law,

$$\frac{\partial c_i(t,0)}{\partial y} = \frac{s_i i}{nFD_i} \ . \qquad \text{[A-4]}$$

The solution, often referred to as the Sand equation, is

$$c_i^{surf} - c_i^{\infty} = -\frac{2s_i i}{nF}\left(\frac{t}{\pi D_i}\right)^{\frac{1}{2}} \ . \qquad \text{[A-5]}$$

Using equation [A-5], Duhamel's integral can be written for the SPE system with a time-varying current source:

$$c_i^{surf} - c_i^{\infty} = -\int_0^t i(\lambda)\frac{d}{d\lambda}\left[-\frac{2s_i}{nF}\left(\frac{t-\lambda}{\pi D_i}\right)^{\frac{1}{2}}\right]d\lambda \qquad \text{[A-6]}$$

or

$$c_i^{surf} - c_i^{\infty} = -\frac{s_i}{nF\sqrt{\pi D_i}}\int_0^t i(\lambda)(t-\lambda)^{-\frac{1}{2}} \ , \qquad \text{[A-7]}$$

which is Eq. [7] of the text. The development of an integral analogous to Eq. [A-7]

for the RDE system is easily accomplished by a similar derivation.

The Coefficients and Eigenvalues for Eq. [23]

The following table gives the first ten eigenvalues b_k and coefficients B_k. Reference 15 or 23 should be consulted for the eigenfunctions $Z_k(\zeta)$.

Table A-1. Coefficients and Eigenvalues for Eq. [23]

k	B_k	b_k
0	0.663516066	2.58078493
1	0.081564022	12.3099728
2	0.034457046	24.4331401
3	0.01962199	38.3054830
4	0.0128965	53.5740271
5	0.0092267	70.0220380
6	0.0069829	87.5010784
7	0.0055048	105.902059
8	0.0044654	125.140833
9	0.0037089	145.15016

The Newton-Raphson Algorithms

For both current-potential expressions, E is solved for by a Newton-Raphson algorithm.

The One-Step Reaction Scheme

The function $H(E)$ is defined by

$$H = i(t) - i(E) \ . \qquad \text{[A-8]}$$

The cell-current density $i(t)$ is known. The second term $i(E)$ is given by the right side of Eq. [28]. For the correct value of E, H will be zero. The potential E (equal to V in Eq. [27] since a SHE reference is assumed and the ohmic drop is neglected) can be found by iteration:

$$E_{new} = E_{old} - \left.\frac{H}{\left(\frac{dH}{dE}\right)}\right|_{old} \qquad \text{[A-9]}$$

The derivative $\frac{dH}{dE}$ is

$$\frac{dH}{dE} = k_a(1-\beta)nfe^{(1-\beta)nfE} + k_c\beta nfe^{-\beta nfE}\frac{c^{surf}_{Cd^{2+}}}{\rho_o} \; . \qquad \text{[A-10]}$$

The Two-Step Reaction Scheme

Making use of Eq. [32], the function H is defined as

$$H = w_1e^{w_2E} + w_3e^{w_4E} + w_5e^{w_6E} + w_7e^{w_8E} \; . \qquad \text{[A-11]}$$

The new variables are:

$$w_1 = k_{c1}k_{c2}exp(-2fU^{\theta})$$

$$w_2 = (2-\beta_1-\beta_2)f$$

$$w_3 = k_{c1}k_{c2}\frac{c^{surf}_{Cd^{2+}}}{\rho_o}$$

$$w_4 = -(\beta_1+\beta_2)$$

$$w_5 = -\frac{i}{2F}k_{c2}$$

$$w_6 = -\beta_2 f$$

$$w_7 = -\frac{i}{2F}k_{c1}exp(-fU^{\theta}_1)$$

$$w_8 = (1-\beta_1)f$$

The value of U^{θ} is $-0.403\,volts$ for this system. The derivative $\frac{dH}{dE}$ is

$$\frac{dH}{dE} = w_1w_2e^{w_2E} + w_3w_4e^{w_4E} + w_5w_6e^{w_6E} + w_7w_8e^{w_8E} \; . \qquad \text{[A-12]}$$

Equations [A-9],[A-11], and [A-12] can be used to solve for E.

References

1. *Standard Math Tables*, W.H. Beyer, Editor, CRC Press, Cleveland, Ohio, 1973, p. 406.
2. A.C. Testa and W.H. Reinmuth, *Anal. Chem.*, 33(1961)1325.
3. R.W. Murray and C.N. Reilley, *J. Electroanal. Chem.*, 3(1962)64.
4. R.W. Murray and C.N. Reilley, *ibid.*, 3(1962)182.
5. W.H. Reinmuth, *Anal. Chem.*, 34(1962)1446.
6. H.B. Herman and A.J. Bard, *ibid.*, 35(1963)1121.
7. H.B. Herman and A.J. Bard, *ibid.*, 36(1964)510.
8. M. Paunovic, *J. Electroanal. Chem.*, 14(1967)447.
9. R.K. Jain, H.C. Gaur, and B.J. Welch, *ibid.*, 79(1977)211.
10. *Handbook of Mathematical Functions*, M. Abramowitz and I.A. Stegun, Editors, Dover Publications, Inc., New York, 1972, pp. 300-302.
11. T.R. Rosebrugh and W. Lash Miller, *J. Phys. Chem.*, 14(1910)816.
12. V.S. Krylov and V.N. Babak, *Sov. Electrochem.*, 7(1971)626; (*Elektrokhimiya*, 7(1971)649).
13. J.S. Newman, *J. Electrochem. Soc.*,113(1966)1235.
14. B. Miller and S. Bruckenstein, *ibid.*,117(1970)1032.
15. K.M. Nisancioglu and J.S. Newman, *J. Electroanal. Chem.*, 50(1974)23.
16. K. Viswanathan, M.A. Farrel Epstein, and H.Y. Cheh, *J. Electrochem. Soc.*, 125(1978)1772.
17. D.A. Scherson, P.F. Marconi, and J.S. Newman, *ibid.*, 127(1980)2603.
18. P.C. Andricacos and H.Y. Cheh, *J. Electroanal. Chem.*, 121(1981)133.
19. D-T. Chin, *J. Electrochem. Soc.*, 130(1983)1657.
20. A.M. Pesco and H.Y. Cheh, *ibid.*, 131(1984)2259.

21. W.G. Cochran, *Proceedings of the Cambridge Philosophical Society*, 30(1934)365.

22. J.S. Newman, *Electrochemical Systems*, Prentice-Hall, Inc., Englewood Cliffs, NJ, 1973.

23. K.M. Nisancioglu, *Ph.D. Thesis*, University of California, Berkeley, 1973.

24. K.J. Vetter, *Electrochemical Kinetics*, S. Bruckenstein and B. Howard, Translation Editors, Academic Press, New York, 1967.

25. A.R. Despic, D.R. Jovanovic, and S.P. Bingulac, *Electrochim. Acta*, 15(1970)459.

26 V.V. Losev, *Modern Aspects of Electrochemistry*, B.E. Conway and J.O'M. Bockris, editors, Plenum Press, New York, 1972, pp. 314-398.

27. J.N. Jovicevic, A.R. Despic, and D.M. Drazic, *Electrochim. Acta*, 22(1977)577.

28. J.A. Harrison and D.R. Sandbach, *J. Electroanal. Chem.*, 85(1977)125.

29. L. Kisova, M. Goledzinowski, and J. Lipkowski, *ibid.*, 95(1979)29.

30 C.P.M. Bongenaar, A.G. Remijnse, M. Sluyters-Rehbach and J.H. Sluyters, *ibid.*, 111(1980)139.

31 C.P.M. Bongenaar, A.G. Remijnse, E. Temmerman, M. Sluyters-Rehbach, and J.H. Sluyters, *ibid.*, 111(1980)155.

32. K. Levenberg, *Quart. Appl. Math.*, 2(1944)164.

33. D.W. Marquardt, *J. Soc. Indust. Appl. Math.*, 11(1963)431.

34. B.S. Garbow, K.E. Hillstrom, and J.J. More, Argonne National Laboratory, March 1980.

35. J.A. Nelder and R. Mead, *The Computer Journal*, 7(1965)308.

36. M.S. Caceci and P. Cacheris, *BYTE*, May 1984, p.340.

37. W. Lorenz, *Z. Electrochem.*, 58(1954)912.

Figure Captions

Fig. 1. Periodic Current Source. For the experiments in this work, $i_I = 0$ and $i_{II} = -1.53\ \frac{mA}{cm^2}$.

Fig. 2. The Dimensionless Concentration for the SPE. The periodic solution is represented by the wavy, solid curve. The dotted curve results if only the $j = 1$ term is retained in the series. The solid, monotonic curve represents the SPE solution if the current were stepped to $\frac{i_{II}}{2}$. For this plot, $i_I = 0$.

Fig. 3. Limiting Current Curves for Cd^{2+}. The current is swept from 0 $\frac{mA}{cm^2}$ at a rate of $-0.75\ \frac{mA}{min-cm^2}$. From right to left, the curves represent 235, 275, 314, and 392 rpm.

Fig. 4. Levich Plot for Cd^{2+}. These data yield $D_{Cd^{2+}} = 3.6 \times 10^{-6}$.

Fig. 5. Electrode Potential. Dotted curve: experimental data. (235 rpm, 0.01 Hz) Lower, solid curve: optimized model prediction. Upper, solid curve: theoretically calculated potential for no kinetic resistance.

Fig. 6. Electrode Potential. Dotted curve: experimental data. (392 rpm, 0.01 Hz) Lower, solid curve: optimized model prediction. Upper, solid curve: theoretically calculated potential for no kinetic resistance.

Fig. 7. Electrode Potential. Dotted curve: experimental data. (235 rpm, 0.1 Hz) Lower, solid curve: optimized model prediction. Upper, solid curve: theoretically calculated potential for no kinetic resistance.

Fig. 8. Surface Concentration. The $c^{surf}_{Cd^{2+}}$ history during the uniform and sustained periodic state for the conditions of Fig. 7.

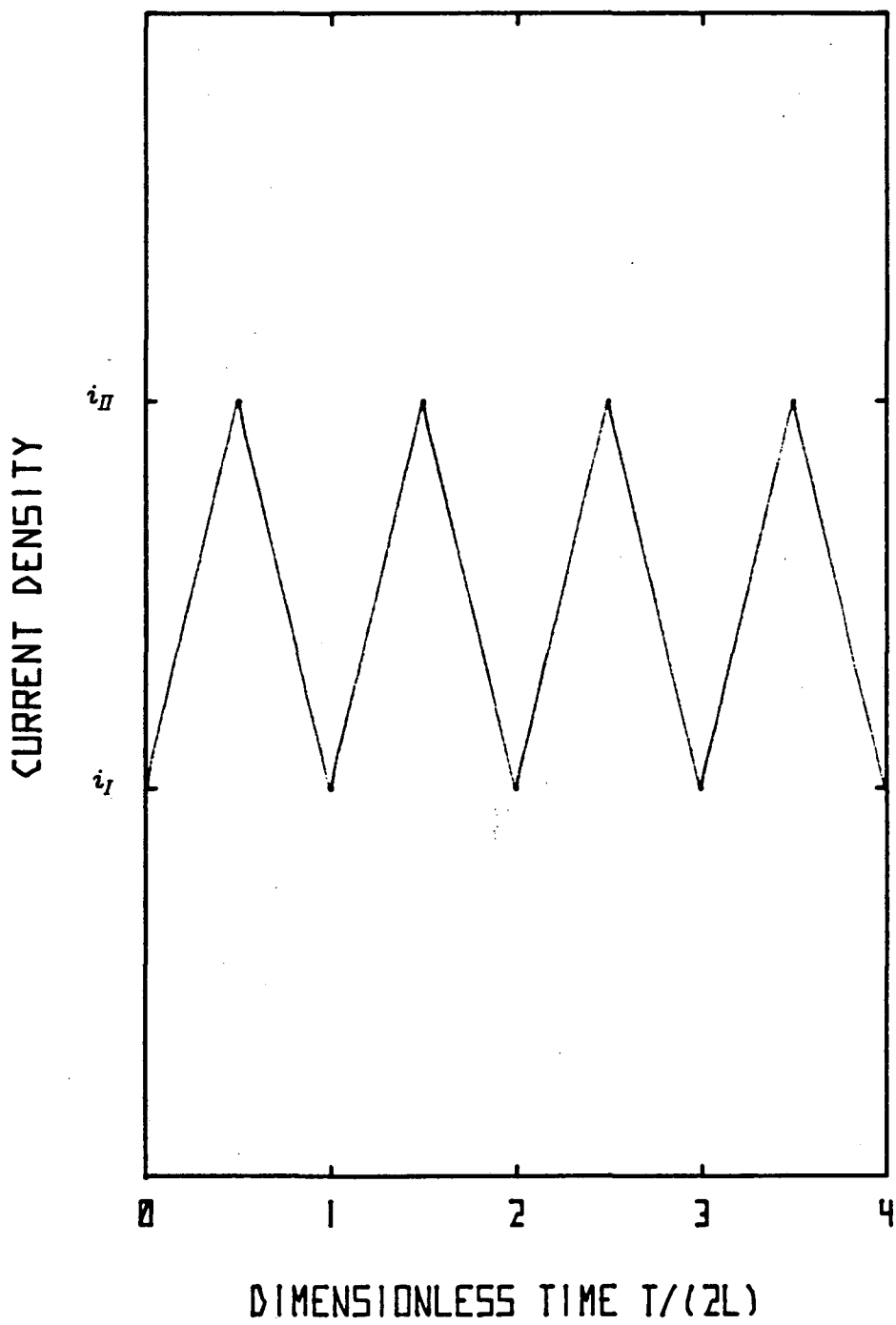

Figure 1.

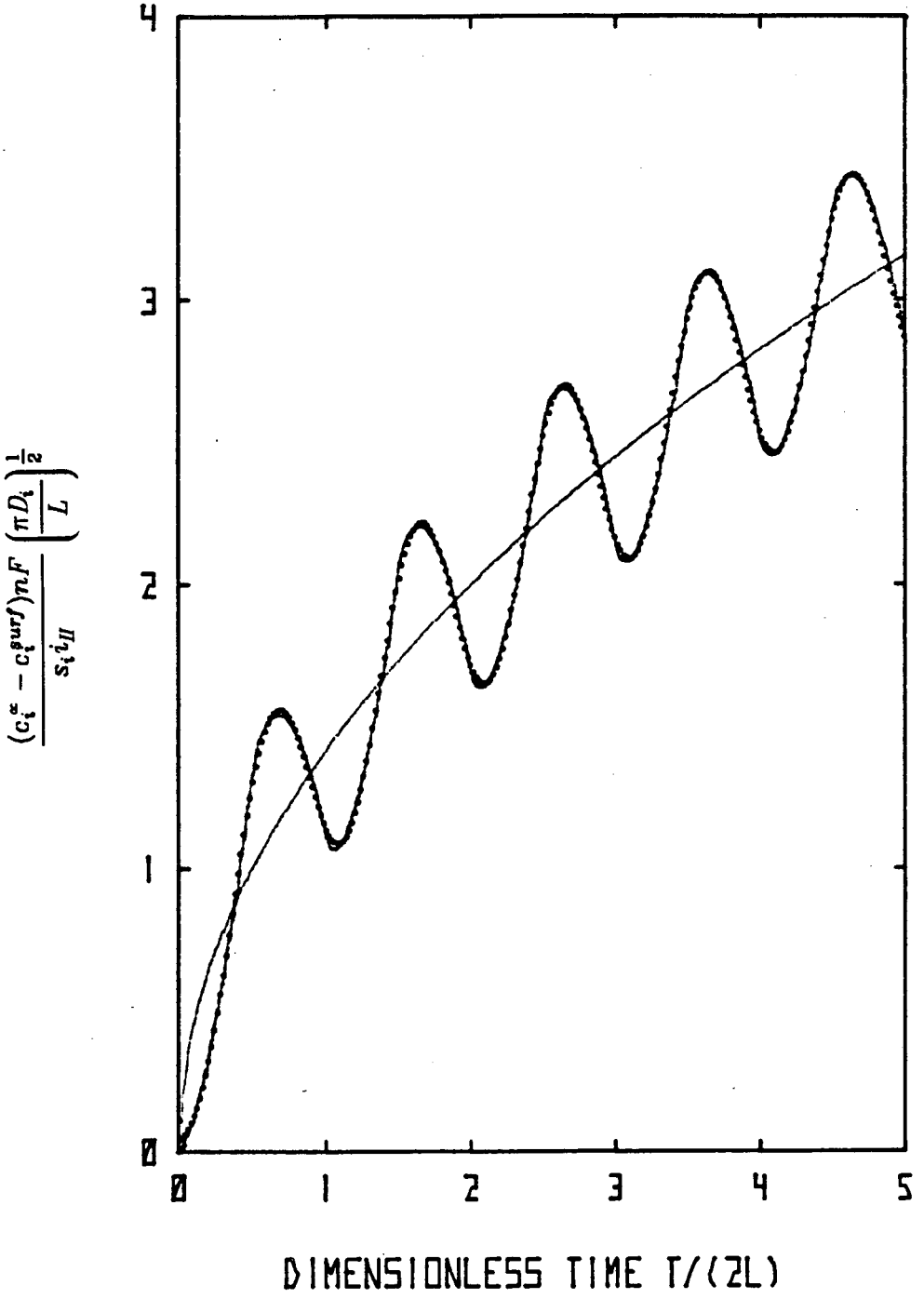
$\frac{(c_i^{\infty} - c_i^{surf})nF}{s_i i_{II}} \left(\frac{\pi D_i}{L}\right)^{\frac{1}{2}}$
0
1
2
3
4
0
1
2
3
4
5
DIMENSIONLESS TIME T/(2L)

Figure 2.

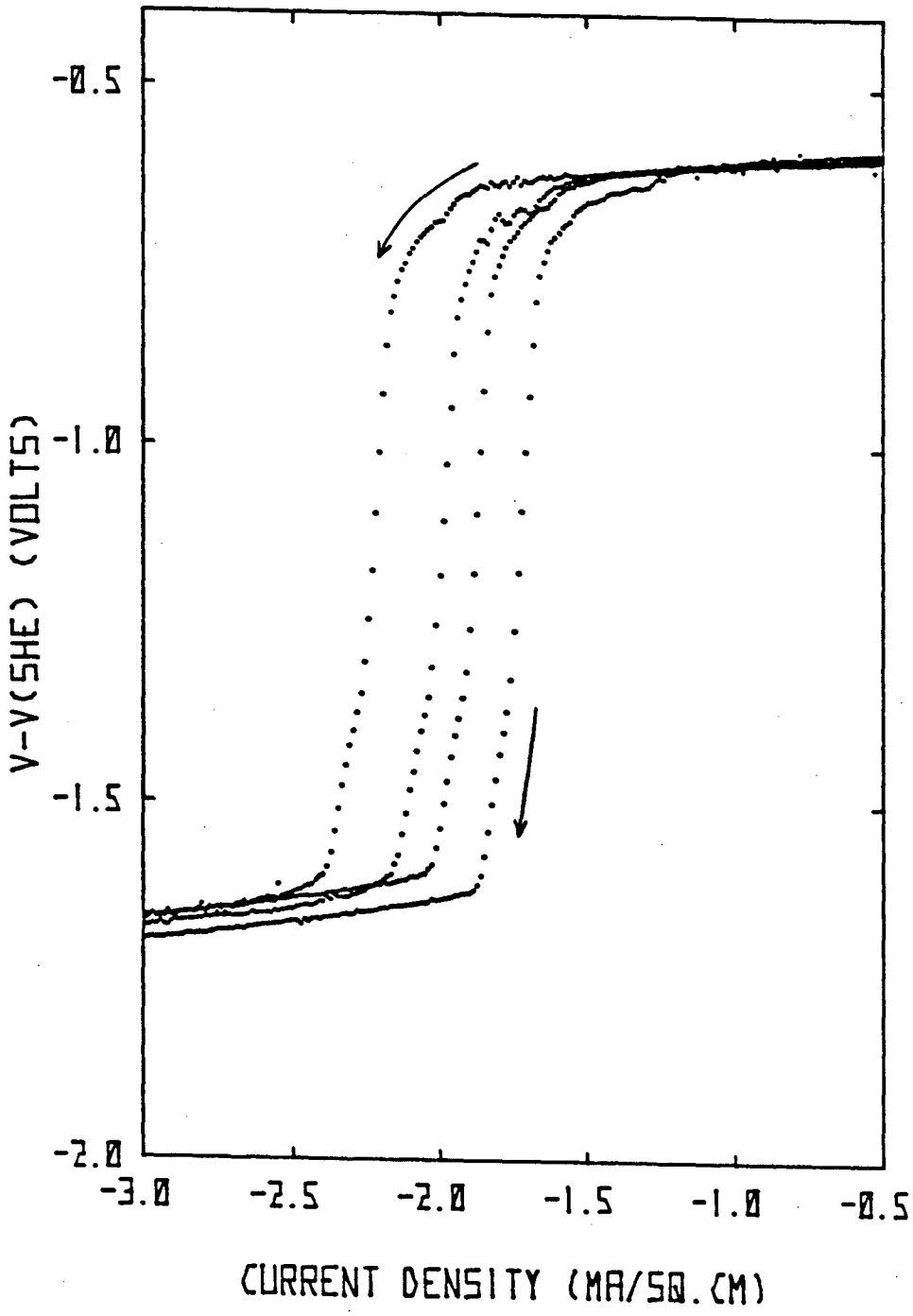
-0.5
-1.0
-1.5
-2.0
V-V(SHE) (VOLTS)
-3.0
-2.5
-2.0
-1.5
-1.0
-0.5
CURRENT DENSITY (MA/SQ.CM)

Figure 3.

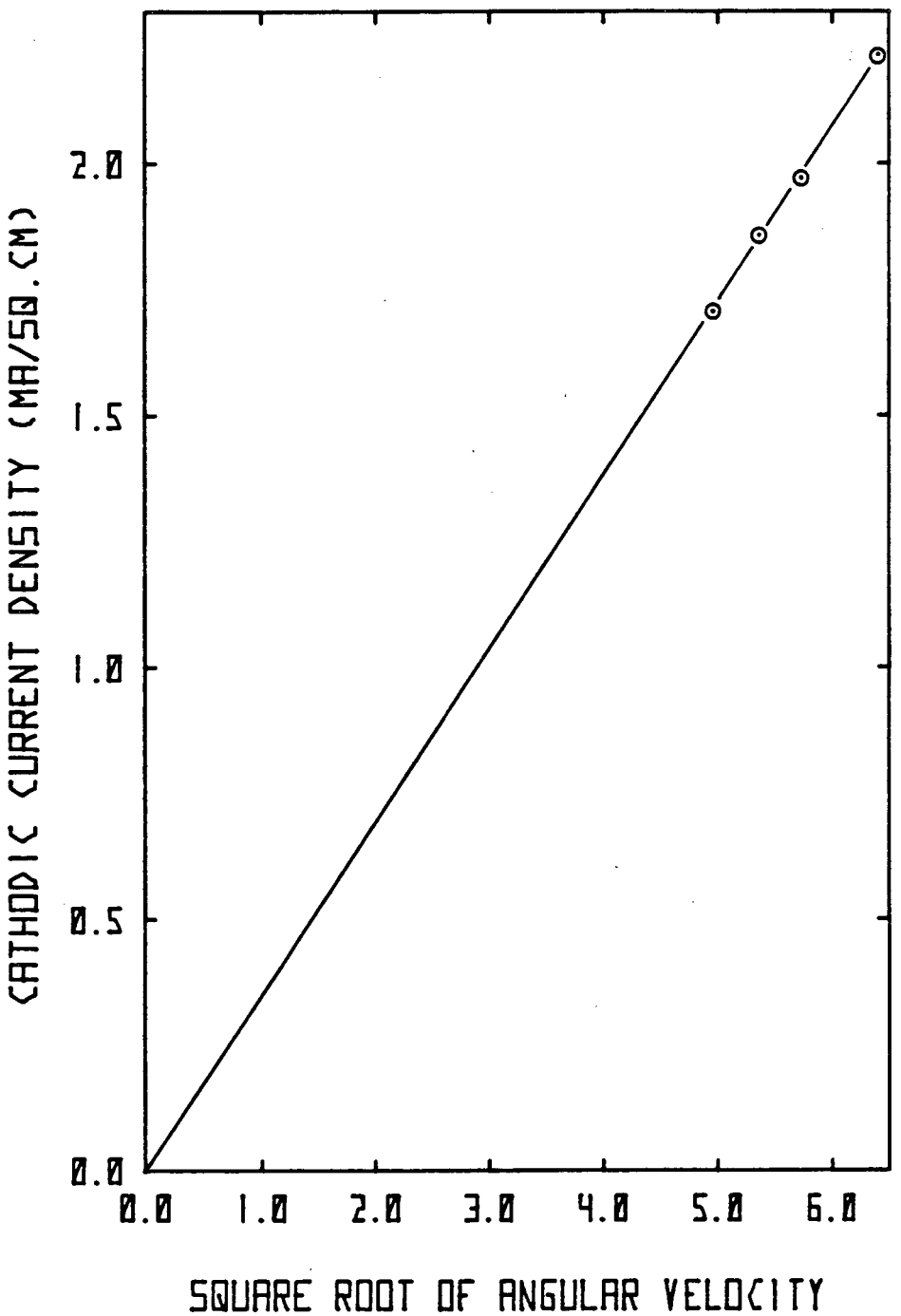
CATHODIC CURRENT DENSITY (MA/SQ.CM)
2.0
1.5
1.0
0.5
0.0
0.0
1.0
2.0
3.0
4.0
5.0
6.0
SQUARE ROOT OF ANGULAR VELOCITY

Figure 4.

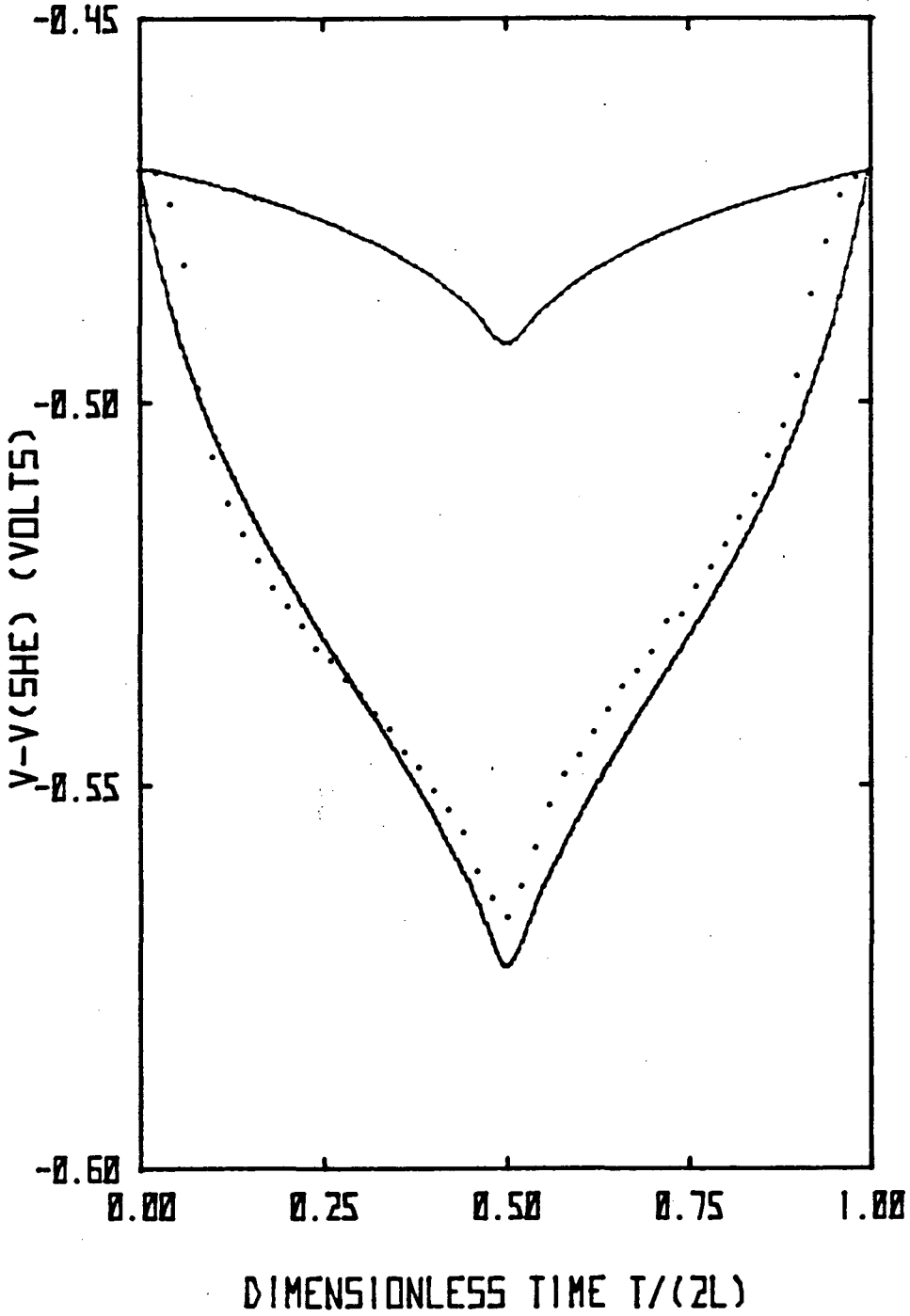
-0.45
-0.50
-0.55
-0.60
V-V(SHE) (VOLTS)
0.00
0.25
0.50
0.75
1.00
DIMENSIONLESS TIME T/(2L)

Figure 5.

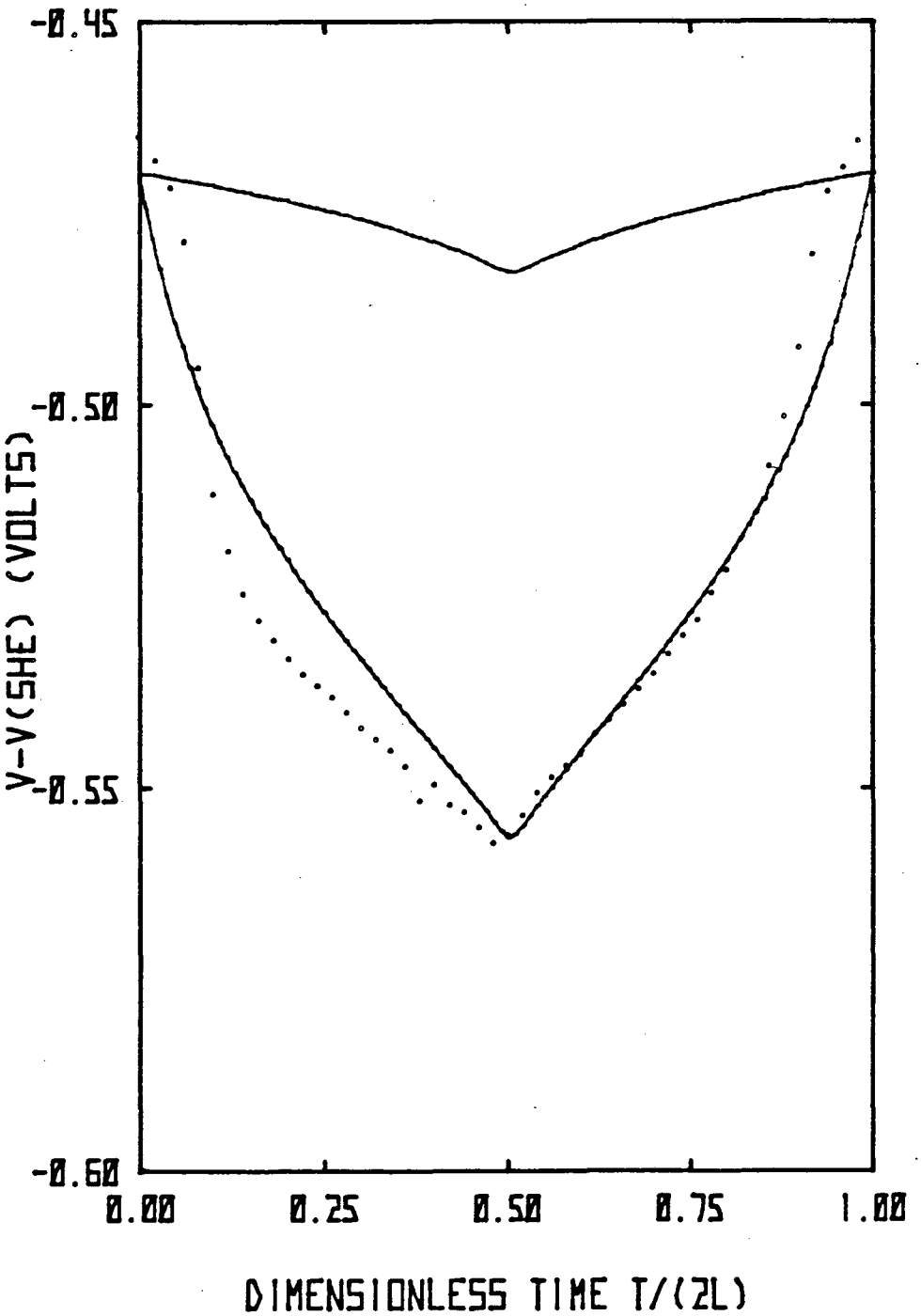
-0.45
-0.50
-0.55
-0.60
V-V(SHE) (VOLTS)
0.00
0.25
0.50
0.75
1.00
DIMENSIONLESS TIME T/(2L)

Figure 6.

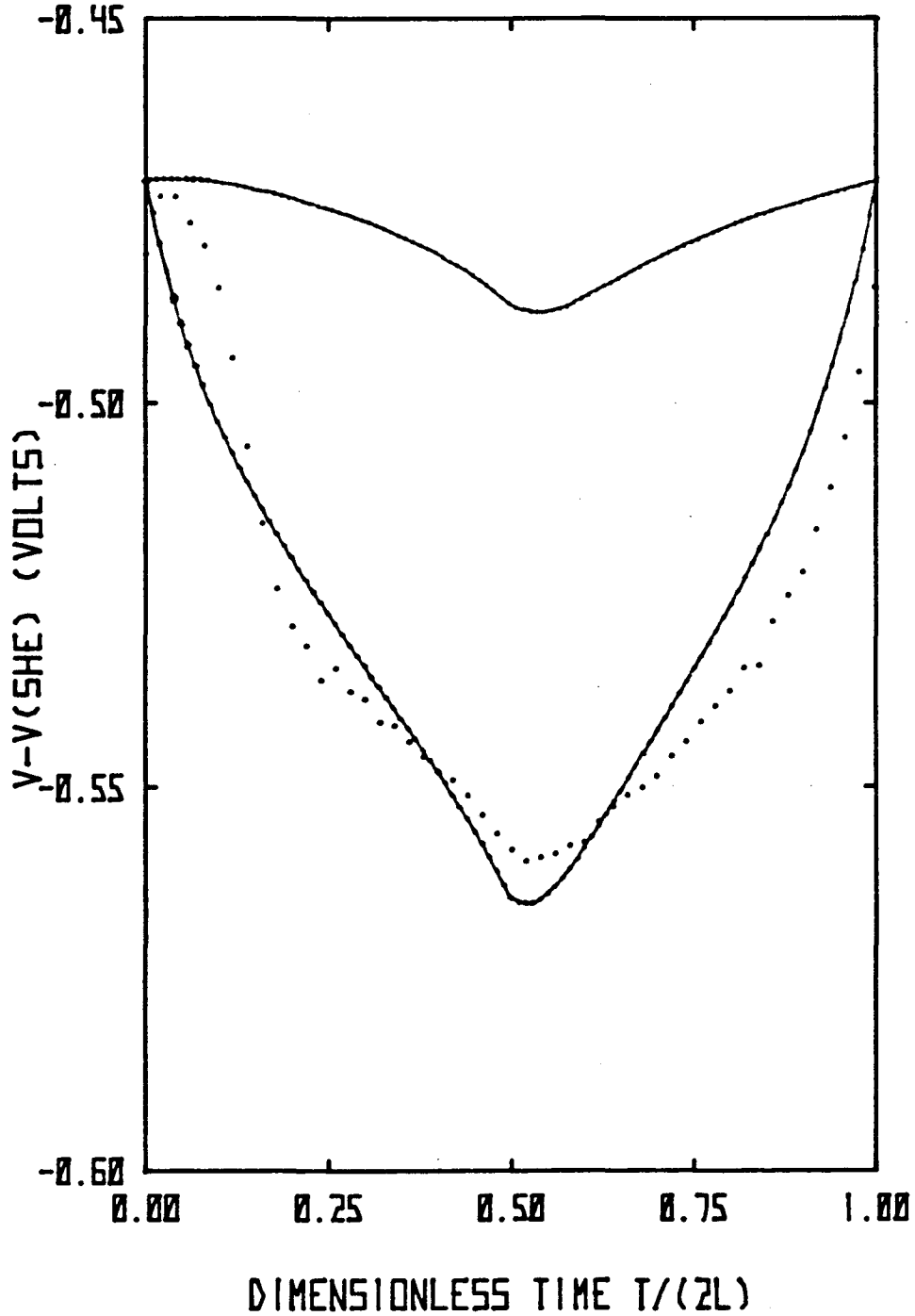
-0.45
-0.50
-0.55
-0.60
V-V(SHE) (VOLTS)
0.00
0.25
0.50
0.75
1.00
DIMENSIONLESS TIME T/(2L)

Figure 7.

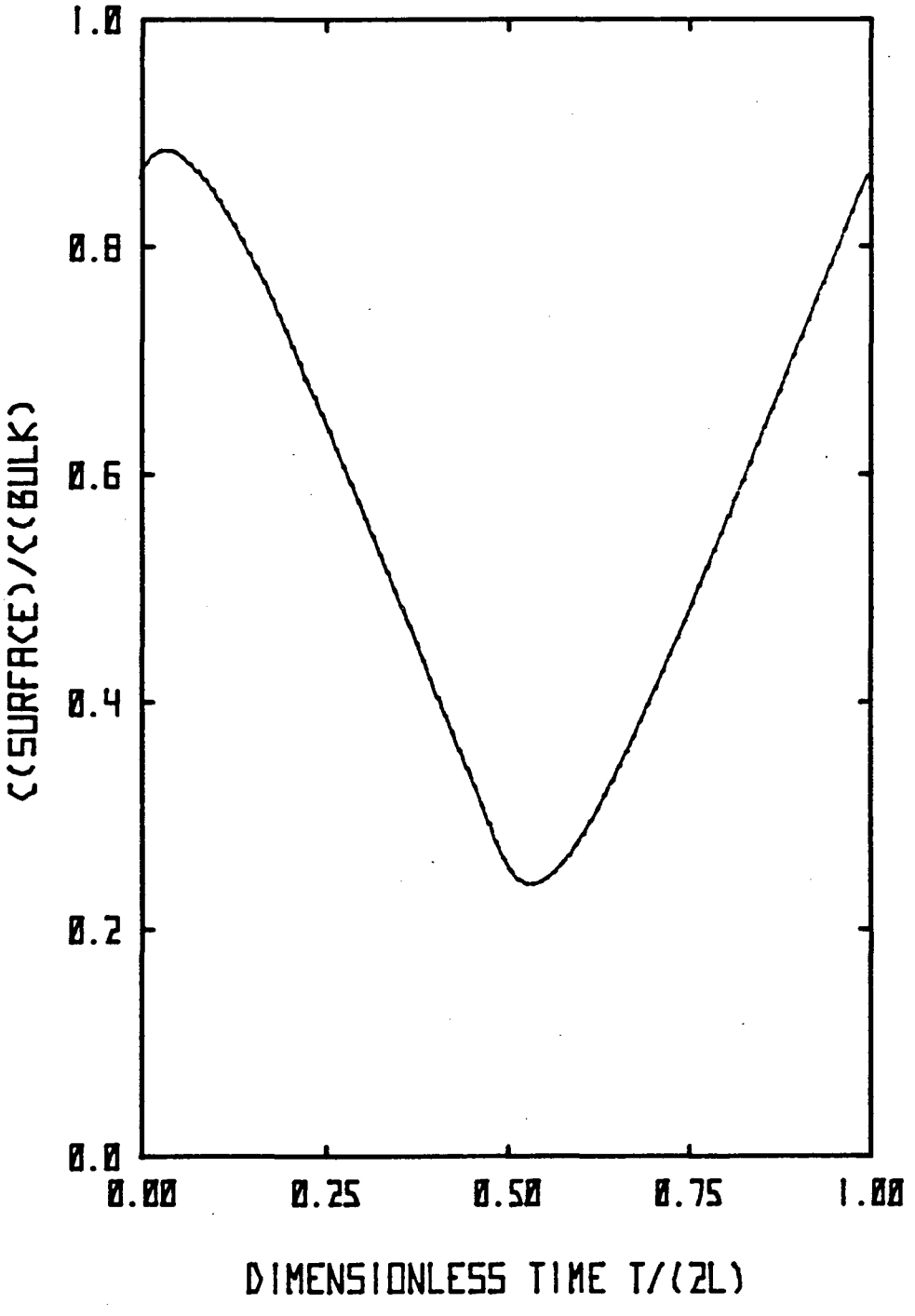
1.0
0.8
0.6
0.4
0.2
0.0
C(SURFACE)/C(BULK)
0.00
0.25
0.50
0.75
1.00
DIMENSIONLESS TIME T/(2L)

Figure 8.

This report was done with support from the Department of Energy. Any conclusions or opinions expressed in this report represent solely those of the author(s) and not necessarily those of The Regents of the University of California, the Lawrence Berkeley Laboratory or the Department of Energy.

Reference to a company or product name does not imply approval or recommendation of the product by the University of California or the U.S. Department of Energy to the exclusion of others that may be suitable.

TECHNICAL INFORMATION DEPARTMENT
LAWRENCE BERKELEY LABORATORY
UNIVERSITY OF CALIFORNIA
BERKELEY, CALIFORNIA 94720